Science of the Total Environment 881 (2023) 163465

Contents lists available at ScienceDirect

Science of the Total Environment

journal homepage: www.elsevier.com/locate/scitotenv

Integrating CRISPR-Cas12a with catalytic hairpin assembly as a logic gate biosensing platform for the detection of polychlorinated biphenyls in water samples

Fang Deng [a,b], Jiafeng Pan [a,b], Manjia Chen [b,c], Zhi Liu [a,*], Junhua Chen [b,*], Chengshuai Liu [c,d]

[a] College of Bioscience and Biotechnology, Hunan Agricultural University, Changsha 410128, China
[b] National-Regional Joint Engineering Research Center for Soil Pollution Control and Remediation in South China, Guangdong Key Laboratory of Integrated Agro-environmental Pollution Control and Management, Institute of Eco-environmental and Soil Sciences, Guangdong Academy of Sciences, Guangzhou 510650, China
[c] Guangdong Laboratory for Lingnan Modern Agriculture, Guangzhou 510642, China
[d] State Key Laboratory of Environmental Geochemistry, Institute of Geochemistry, Chinese Academy of Sciences, Guiyang 550081, China

HIGHLIGHTS

- PCB72 and PCB77 were used as the two inputs to construct the logic gate biosensor.
- Hairpin DNA assembly and CRISPR-Cas12a were used in the logic sensing system.
- YES, OR, AND, and INHIBIT logic gates were successfully fabricated.
- The logic gates can realize the intelligent sensing of PCBs in complex samples.

GRAPHICAL ABSTRACT

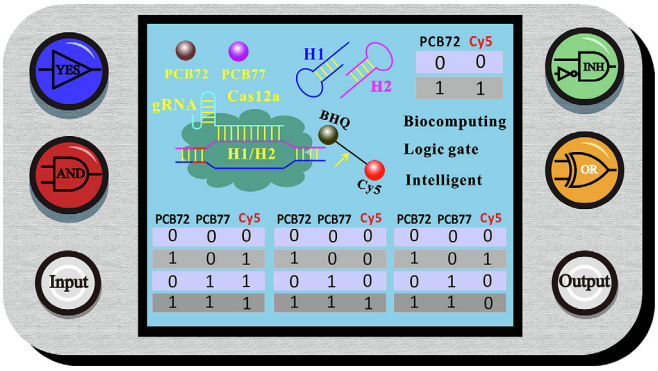

ARTICLE INFO

Editor: Damia Barcelo

Keywords:
Logic gate
CRISPR-Cas12a
Polychlorinated biphenyl
Catalytic hairpin assembly
Intelligent detection

ABSTRACT

Polychlorinated biphenyls (PCBs) are ubiquitous persistent organic pollutants that cause harmful effects on environmental safety and human health. There is an urgent need to develop an intelligent method for PCBs sensing. In this work, we proposed a logic gate biosensing platform for simultaneous detection of multiple PCBs. 2,3′,5,5′-tetrachlorobiphenyl (PCB72) and 3,3′,4,4′-tetrachlorobiphenyl (PCB77) were used as the two inputs to construct biocomputing logic gates. We used 0 and 1 to encode the inputs and outputs. The aptamer was used to recognize the inputs and release the trigger DNA. A catalytic hairpin assembly (CHA) module is designed to convert and amplify each trigger DNA into multiple programmable DNA duplexes, which initiate the *trans*-cleavage activity of CRISPR/Cas12a for the signal output. The activated Cas12 cleaves the BHQ-Cy5 modified single-stranded DNA (ssDNA) to yield the fluorescence reporting signals. In the YES logic gate, PCB72 was used as the only input to carry out the logic operation. In the OR, AND, and INHIBIT logic gates, PCB72 and PCB77 were used as the two inputs. The output signals can be visualized by the naked eye under UV light transilluminators or quantified by a microplate reader. Our constructed biosensing platform possesses the merits of multiple combinations of inputs, intuitive digital output, and high flexibility and scalability, which holds great promise for the intelligent detection of different PCBs.

* Corresponding authors.
E-mail addresses: tigerzhiliu@126.com (Z. Liu), 222chenjunhua@163.com (J. Chen).

http://dx.doi.org/10.1016/j.scitotenv.2023.163465
Received 8 February 2023; Received in revised form 23 March 2023; Accepted 8 April 2023
Available online 15 April 2023

1. Introduction

Polychlorinated biphenyls (PCBs) are a class of synthetic organic compounds with high toxicity, poor degradation, long-term stability, and bioaccumulation properties (Andrew et al., 2022; Melymuk et al., 2022). Among the PCBs, 2,3′,5,5′-tetrachlorobiphenyl (PCB72) and 3,3′,4,-4′-tetrachlorobiphenyl (PCB77) are widely distributed in water and soil samples. Even trace amounts of them can cause harmful effects on the environmental and food safety (Christensen et al., 2021; Lammel et al., 2019). Traditional techniques for PCB detection focused on gas chromatography–mass spectrometry (GC–MS) and high-performance liquid chromatography-mass spectrometry (HPLC-MS) (Gao et al., 2020; Zhang et al., 2022). Although they are sensitive and accurate, the requirement of sophisticated equipment and complex pre-treatment steps limited their wide applications for the routine monitoring of PCBs (Xu et al., 2021). Recently, some elegant biosensors have been developed for PCB detection using electrochemical (Fan et al., 2019; Sun et al., 2019; Zhang et al., 2021), fluorescence (Wang et al., 2018), and colorimetric methods (Cheng et al., 2018; Chen et al., 2021). Those sensors have made great progress in PCB monitoring. However, to the best of our knowledge, there are very few reports on the intelligent detection of PCBs. Thus, the construction of an intelligent sensing system for PCBs assay is still challenging and interesting.

As an effective way to realize the intelligent sensing, molecular logic gate has attracted a lot of attention in biological imaging (Erbas-Cakmak et al., 2018; Tregubov et al., 2018), disease diagnosis (Feng et al., 2020), and biosensor assay (Yi et al., 2021). In molecular logic gate design, 0 and 1 are often used to encode the inputs and outputs. The presence and absence of the inputs are defined as 1 and 0, respectively (Ge et al., 2016; Wang et al., 2020). The output signals below or above a threshold value are set as 0 and 1, respectively. Some interesting logic gates have been reported for nucleic acid, metal ion, and protein sensing using OR, AND, XOR, NAND, NOR, and INHIBIT logic operations (Miao and Tang, 2021; Deng et al., 2023; Chen et al., 2020; Yu et al., 2021). There are few attempts to develop logic gate using toxic organic pollutants as inputs. Thus, it is highly desirable to explore the new applications of molecular logic gates in organic pollutant biosensing, especially using PCB72 and PCB77 as inputs.

As a powerful gene editing tool, the clustered regularly interspaced short palindromic repeats (CRISPR)-Cas (CRISPR-associated) system has attracted great interest in biosensor design (Dronina et al., 2021a, 2021b). CRISPR-Cas12a is a type of CRISPR-Cas system composed of guide RNA (gRNA) and Cas12a nuclease. CRISPR-Cas12a is an RNA-guided endonuclease with trans-cleavage activity (Dronina et al., 2022; Kaminski et al., 2021; Li et al., 2018). Upon recognition of the protospacer adjacent motif (PAM) site in the double-stranded DNA (dsDNA), the Cas12a will be activated to cleave the single-stranded DNA (ssDNA) nonspecifically (Tang et al., 2021; Feng et al., 2021). Such unique characteristics make CRISPR-Cas12a as a promising candidate to fabricate electrochemical sensors (Li et al., 2018; Shen et al., 2021), fluorescence detectors (Pan et al., 2023; Yue et al., 2021; Nguyen et al., 2020; Xiong et al., 2020; Li et al., 2021), colorimetric biosensors (Zhou et al., 2020; Ding et al., 2020; Jiang et al., 2021), and lateral flow strips (Xiong et al., 2021; Cao et al., 2022; Liu et al., 2022). In this work, we attempt to design a logic platform for the intelligent detection of PCBs using CRISPR-Cas12a as the signal conversion tool. PCB72 and PCB77 were used as the two inputs and fluorescence signals were used as the outputs. The PCB-aptamer binding will trigger the hairpin probe assembly in the system to generate numerous dsDNA, which can be recognized by Cas12a. Through the rational design of the sensing DNA probes, the YES, OR, AND, and INHIBIT logic gates were successfully constructed.

2. Experimental section

2.1. Materials and reagents

All HPLC-purified DNA probes were purchased from Sangon Biotech Co., Ltd. (Shanghai, China) and their sequences were listed in Tables S1-S4 (Supporting Information).

PCBs were purchased from Aladdin Biochemical Technology Co. Ltd. (Shanghai, China). EnGen Lba Cas12a (Cpf1) and 10 × NEBuffer™ 2.1 Buffer were purchased from New England Biolabs Ltd. (Whitby, ON, Canada). Other reagents were of analytical grade and obtained from Sigma-Aldrich (St. Louis, Mo). The buffer was prepared using Milli-Q water (18.2 MΩ/cm).

2.2. Logic computing operations

All DNA probes were dissolved in 20 mM Tris-HCl buffer (pH 7.5, 140 mM NaCl, 5 mM KCl). The Cas12a was dissolved in 1 × NEB buffer™ 2.1. gRNA solution was prepared using DEPC (diethyl pyrocarbonate) treated water. DNA3 were dissolved in the cleavage buffer (20 mM Tris-HCl, pH 7.5, 100 mM KCl, 5 mM $MgCl_2$, 5 % glycerol, and 1 mM DTT). In the YES logic gate, 200 nM DNA1 and 100 nM DNA2 were incubated at room temperature for 15 min. 50 ng/mL PCB72, 400 nM H1, and 400 nM H2 were added and incubated for 60 min at room temperature. 75 nM Cas12a, 100 nM gRNA, and 400 nM DNA3 were added and incubated for 55 min at room temperature. Then, the fluorescence spectra were recorded from 650 to 700 nm (*Ex* = 625 nm, *Em* = 665 nm) by a SpectraMax i3x (Molecular Devices, USA). In the OR, AND, and INHIBIT logic gate, 50 ng/mL PCB72 and PCB77 were used as the inputs. 100 nM H1, 400 nM H2, and 400 nM H3 were used in the logic system. Other procedures were the same as the YES logic gate. The logic results were observed by the naked eye under UV light and the photos were taken with an iPhone equipped with a wide camera.

2.3. Polyacrylamide gel electrophoresis (PAGE) analysis

The details of the PAGE procedures were listed in the Supporting Information.

3. Results and discussion

3.1. Design of 'YES logic gate' based structure

We first employed PCB72 as the model target to construct a YES logic gate (Fig. 1). The absence and presence of the target were defined as 0 and 1, respectively. The trigger DNA (DNA2) was blocked by DNA1. In the presence of PCB72, the specific binding between the aptamer (DNA1) and PCB72 will release the blocked DNA2. The free DNA2 thus can be used as the trigger DNA to initiate the CHA cycle amplification reaction. The hairpin probe 1 (H1) can be opened by the hybridization with DNA2 through toehold-mediated strand displacement. In the formed DNA2-H1 complex, the exposed 3′-overhang in H1 can serve as a new toehold to open hairpin probe 2 (H2) through toehold-mediated strand displacement. The DNA2-H1-H2 is unstable and DNA2 will be liberated from the H1-H2 duplex through branch migration. DNA2 then can be recycled to activate other H1 and H2 for generating numerous H1-H2 dsDNA. The PAM site (yellow) and the protospacer sequence in H1-H2 can be recognized by the Cas12a/gRNA complex. The activated Cas12a can cleave ssDNA (DNA3, modified with BHQ and Cy5) to give out a high fluorescence signal, which can be used to monitor the logic functions. In the absence of PCB72, the trigger DNA was blocked by DNA1. The CHA reaction between H1 and H2 cannot happen. Thus, only background fluorescence signal can be observed. The logic results can be visualized by the naked eye under UV light transilluminators or quantified by a microplate reader (Fig. 2a and b). As shown in Fig. 2b, the input of 1 generates an output of 1 and the input of 0 generates an output of 0. The fluorescence spectra and the corresponding fluorescence intensities at 665 nm of the YES logic gate were shown in Fig. 2c and d.

As the hairpin DNA assembly is important for the construction of the logic gate, we used PAGE experiments to verify the feasibility of the assembly process between H1 and H2. As shown in Fig. S1 (Supporting Information), the bands in lanes 1 and 2 corresponded to H1 and H2, respectively. When DNA2 was mixed with H1 (lane 3), a new band at a higher electrophoresis distance was observed, confirming that DNA2 has opened H1

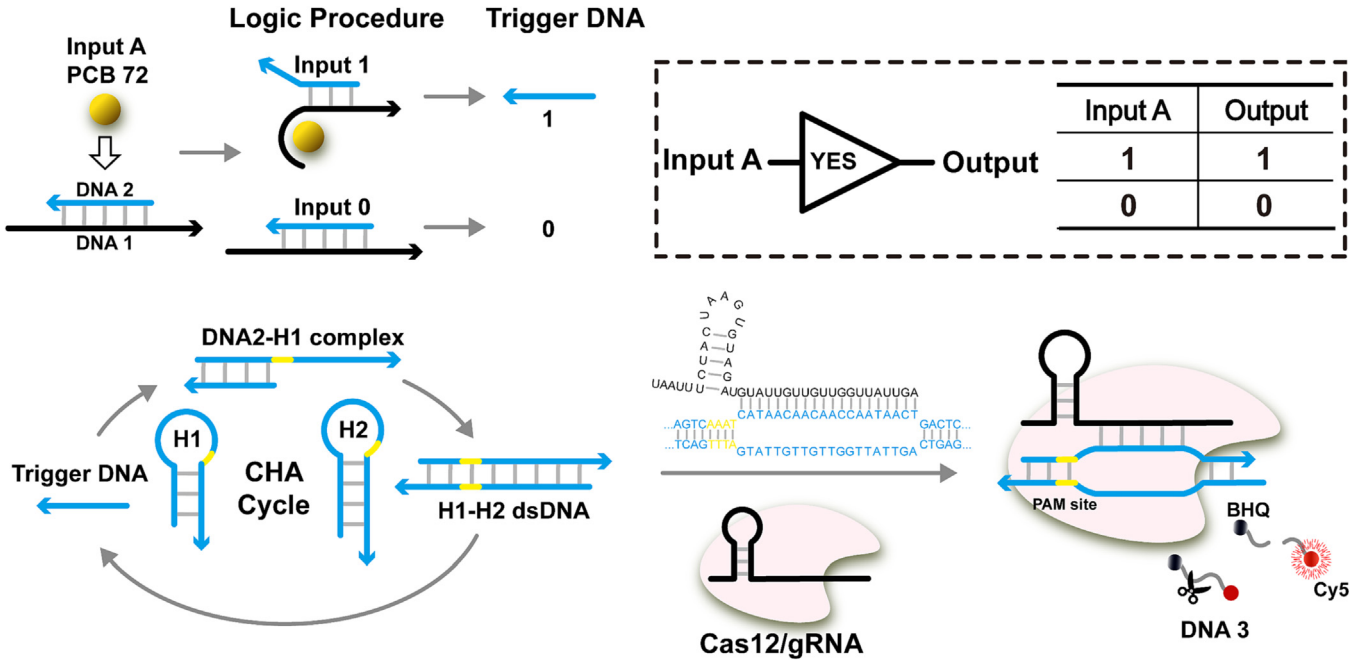

Fig. 1. Schematic illustration of the YES gate using PCB72 as the input. The aptamer (DNA1) was used to recognize the input. Two hairpin probes (H1 and H2) were used to assemble H1/H2 dsDNA. Cas12/gRNA complex was used to cleave the ssDNA (DNA3, modified with BHQ and Cy5) to yield the fluorescence output. Inset: The truth table of the YES logic gate.

and DNA2-H1 duplex was formed. When H2 was introduced, H2 will displace DNA2 to form the H1-H2 duplex. Also, DNA2 will be released (lane 4). Those results successfully verified the assembly reaction between H1 and H2.

We used the YES logic gate to test the analytical performance for PCB72 detection. Under the optimal assay conditions (Fig. S2-S4, Supporting Information), the fluorescence signals increased with the increase of PCB72 concentrations from 0 to 500 ng/mL (Fig. 2e). The resulting calibration curve shows that the fluorescence signals are proportional to the logarithm of PCB72 concentrations in the range from 500 fg/mL to 50 ng/mL (Fig. 2f). The detection limit is calculated to be 128 fg/mL based on 3S/N.

Some nontarget substances, including PCB77, PCB101, PCB118, chlorobenzene, parathion-methyl, aflatoxin B1, ochratoxin A, 1,3-diphenylguanidine, norfloxacin, and Pb were used as the interfering molecules to examine the specificity of the logic biosensor. It was reported that the detected maximum concentrations of 1,3-diphenylguanidine, norfloxacin, and Pb in the Pearl River were 40,020 ng/L, 2702 ng/L, and384.06 mg/kg, respectively (Huang et al., 2019; Hu and Cheng, 2013; Zhang et al., 2023). In the specificity experiment, the concentration of PCB72 was set at 50 ng/mL. The concentrations of PCB77, PCB101, PCB118, chlorobenzene, parathion-methyl, aflatoxin B1, ochratoxin A were set at 500 ng/mL. The concentrations of 1,3-diphenylguanidine, norfloxacin, and Pb were set at 40020 ng/L, 2702 ng/L, and384.06 mg/kg, respectively. As shown in Fig. S5 (Supporting Information), a significant fluorescence response can be observed in the presence of PCB72, whereas the control molecules (PCB77, PCB101, PCB118, chlorobenzene, parathion-methyl, aflatoxin B1, ochratoxinA, 1,3-diphenylguanidine, norfloxacin, and Pb) failed to generate obvious fluorescence signals compared with the blank sample. When the controls were mixed with PCB72, a high fluorescence response can be also observed. These results indicated that this YES logic gate exhibited a high selectivity for PCB72 detection. Such excellent selectivity can be ascribed to the specific binding between the aptamer and the input PCB72.

We also evaluated the practical applications of the YES logic gate in real water samples. Different concentrations of PCB72 were added to the PCB72-free water samples (collected from the Pearl River, Guangzhou, China) and detected using the YES logic gate and the GC–MS method. As shown in the Table 1, the recovery values were in the range of 94–106 % and the relative standard deviations (RSD) were in the range of 2.0–6.8 %. At the same time, the concentrations of PCB72 in the spiked water samples were validated by the GC–MS method. The data revealed that no significant difference existed between the biosensor detection and the GC–MS method (Fig. S6, Supporting Information). The relative error (Re) was from −4.4 % to 6.5 %. Those results indicated that the logic gate biosensor is robust and the complex sample matrix will not affect the analytical performance of the logic system.

3.2. Design of 'OR logic gate' based structure

Using PCB72 and PCB77 as the two inputs, we further constructed an OR logic gate (Fig. 3a). PCB72 and PCB77 were defined as input A and input B, respectively. The aptamer sequences and the trigger DNA were marked clearly in Fig. S7 (Supporting Information). In the presence of input A (1,0), DNA1 and PCB72 interactions will release DNA2. DNA2 thus can perform the same role as the YES logic gate to assemble H2 and H3 into H2/H3 dsDNA. After recognition by the Cas12a/gRNA complex, DNA3 will be cleaved to give out a high fluorescence signal (output = 1). In the presence of input B (0,1), H1 and PCB77 interactions will open H1 to expose the trigger DNA sequence(blue), which possesses the same sequence as DNA2. Thus, the opened H1 can also activate the assembly reaction between H2 and H3 to generate the H2/H3 dsDNA and then yield a high fluorescence signal (output = 1). In the presence of both input A and input B (1,1), the free DNA2 and the opened H1 can be obtained simultaneously. The output of this state still reads 1. The fluorescence spectra and the corresponding fluorescence intensities at 665 nm of the OR logic gate were shown in Fig. 3b and c, respectively. The colorimetric signal of the OR logic gate was shown in Fig. 3d. In OR logic operation, as long as any input is present ((0,1), (1,0), and (1,1)), the output reads 1.

3.3. Design of 'AND logic gate' based structure

Fig. 4a described the construction principle of a AND logic gate. PCB72 and PCB77 were defined as input A and input B, respectively. The aptamer sequences and the trigger DNA were marked clearly in Fig. S8 (Supporting

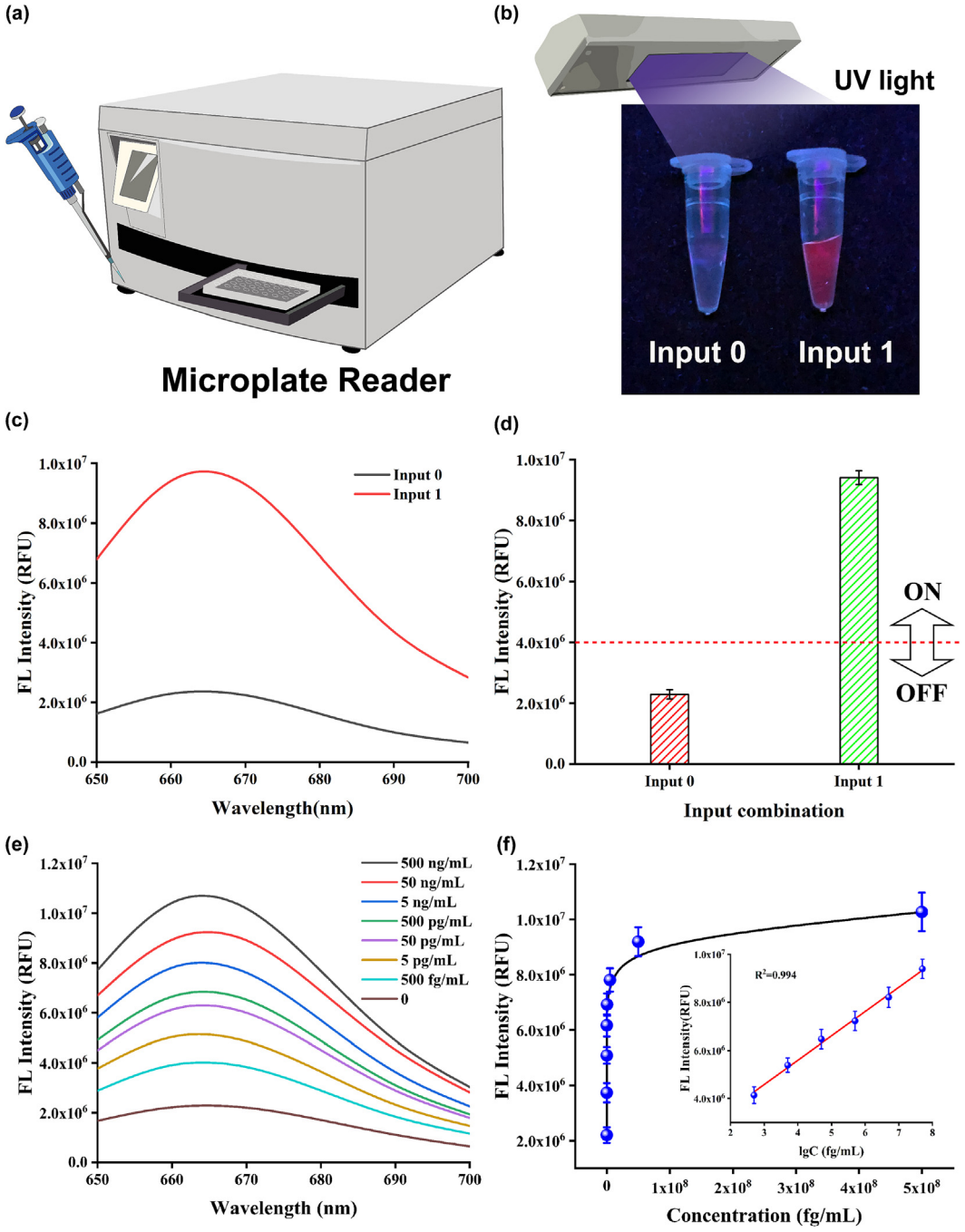

Fig. 2. (a) The output of YES logic gate measured by a microplate reader. (b) The fluorescence colors of the YES logic gate. (c) Fluorescence spectra of the YES logic gate. (d) Column diagram of the corresponding fluorescence intensities at 665 nm. The red dashed line shows the threshold value of 4.0×10^6. (e) Fluorescence spectra of the YES logic gate treated with different PCB72 concentrations. (f) Linear relationship between fluorescence intensities at 665 nm and PCB72 concentrations.

Information). In the presence of input A (1,0), DNA1 and PCB72 interactions will release DNA2. The free DNA2 does not contain the intact trigger DNA, which cannot open H2. Thus, no H2/H3 dsDNA can be formed and the output is 0. In the presence of input B (0,1), H1 and PCB77 interactions will open H1 and expose the looped domain. Similarly, the looped domain does not contain the intact trigger DNA. In this situation, the output still reads 0. In the presence of both input A and input B (1,1), the free DNA2 will hybridize with the opened H1 to form the intact trigger DNA through a-a* binding (green). In DNA2/H1 complex, the intact trigger DNA initiates the toehold-mediated strand displacement to open H2. Through cyclic assembly between H2 and H3, numerous H2/H3 dsDNA were formed. After recognition by Cas12a/gRNA, DNA3 will be cleaved to generate a high fluorescence signal (output = 1). The fluorescence spectra and the corresponding fluorescence intensities at 665 nm of the AND logic gate were shown in Fig. 4b and c, respectively. The colorimetric signal of the AND logic gate was shown in Fig. 4d. In AND logic operation, the output reads 1 only in the presence of both inputs (1,1). Other input combinations ((0,0), (1,0), and (0,1)) generate an output of 0.

3.4. Design of 'INHIBIT logic gate' based structure

We also fabricated an INHIBIT logic gate using PCB72 and PCB77 as the inputs (Fig. 5a). The aptamer sequences and the trigger DNA were marked clearly in Fig. S9 (Supporting Information). In the presence of input A (1,0), the blocked DNA2 will be released due to the PCB72-DNA1 interactions. The free DNA2 can activate the assembly between H2 and H3 to generate

Table 1
Detection of PCB72 in water samples using the proposed biosensor and GC–MS method.

Samples[a]	Added	GC-MS[b]	Our sensor[c]	Recovery (%)	RSD[d] (%)	Re[e] (%)
Water 1#	500 fg/mL	489.16 fg/mL	521.3 fg/mL	104.2	6.8	6.5
Water 2#	5 pg/mL	4.92 pg/mL	4.7 pg/mL	94.0	5.1	−4.4
Water 3#	50 pg/mL	49.87 pg/mL	51.5 pg/mL	103.0	2.0	3.2
Water 4#	500 pg/mL	499.89 pg/mL	508.2 pg/mL	101.64	2.3	1.6
Water 5#	5 ng/mL	5.10 ng/mL	5.3 ng/mL	106.0	5.2	3.9
Water 6#	50 ng/mL	50.03 ng/mL	50.6 ng/mL	101.2	2.4	1.1
Water 7#	500 ng/mL	502.71 ng/mL	518.3 ng/mL	102.0	4.6	3.1

[a] The water samples were collected from the Pearl River, Guangzhou, China.
[b] The concentration of PCB72 in water samples was certified using the gas chromatography–mass spectrometry (GC–MS) method.
[c] The data reported in the table represent the average of three measurements.
[d] RSD: the relative standard deviation.
[e] Re: Our biosensor *vs.* GC–MS method.

H2/H3 dsDNA, which can be recognized by Cas12a/gRNA. After cleavage by Cas12a, DNA3 can yield a high fluorescence signal (output = 1). In the presence of input B (0,1), PCB77 and H1 interactions will open H1 and expose domain a. Domain a is complementary with DNA2. Thus, the output is 0. In the presence of both input A and input B (1,1), the free DNA2 will be blocked again by exposed domain a. Therefore, the DNA2/H2 complex cannot start the assembly between H2 and H3. And the output is 0. The fluorescence spectra and the corresponding fluorescence

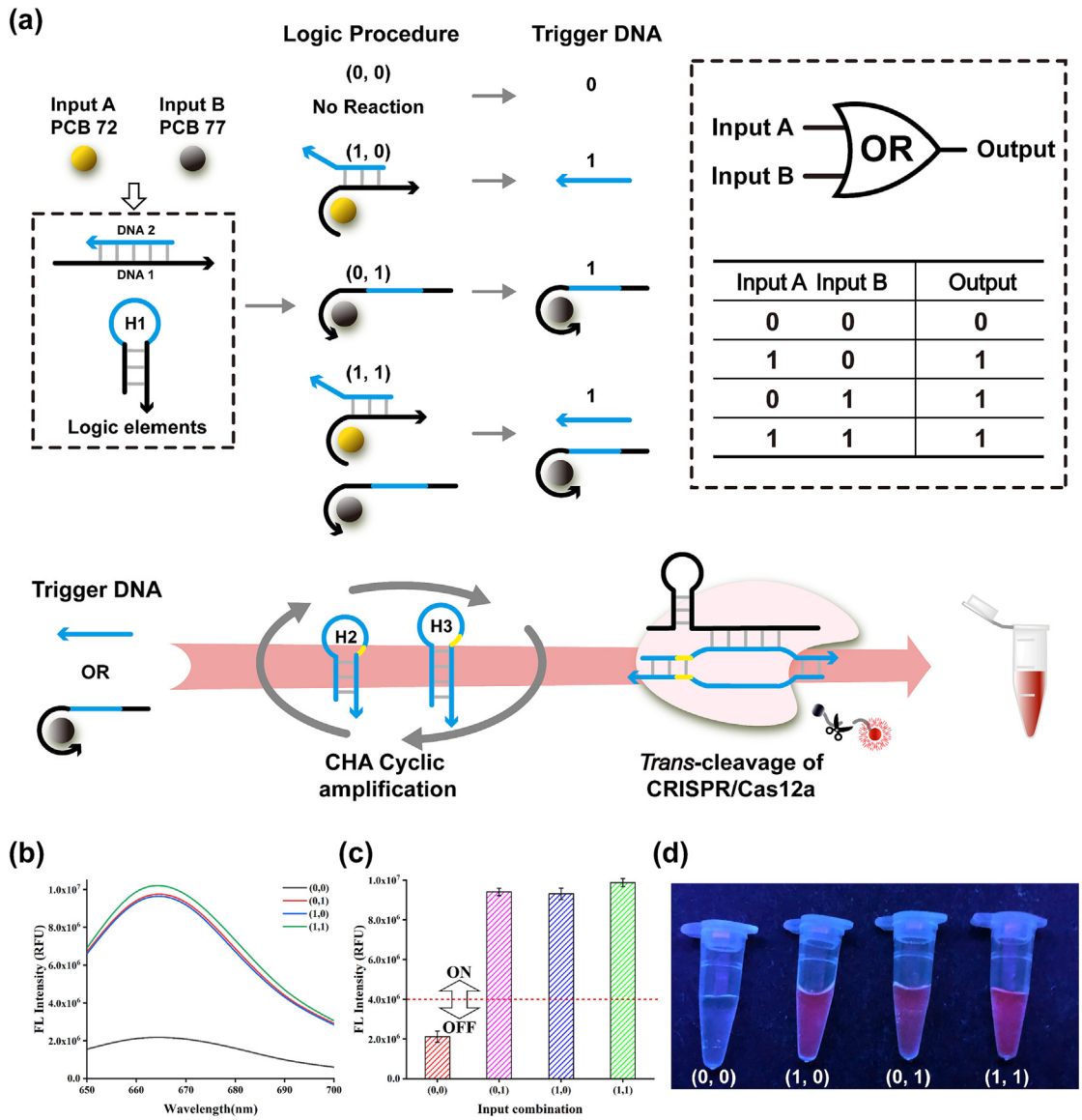

Fig. 3. (a)Schematic illustration of the OR gate using PCB72 and PCB77 as inputs. Inset: The truth table of the OR logic gate. (b) Fluorescence spectra of the OR logic gate. (c) Column diagram of the corresponding fluorescence intensities at 665 nm. The red dashed line shows the threshold value of 4.0×10^6. (d) The colorimetric responses of the OR logic gate with the input combinations of (0,0), (1,0), (0,1), and (1,1), respectively.

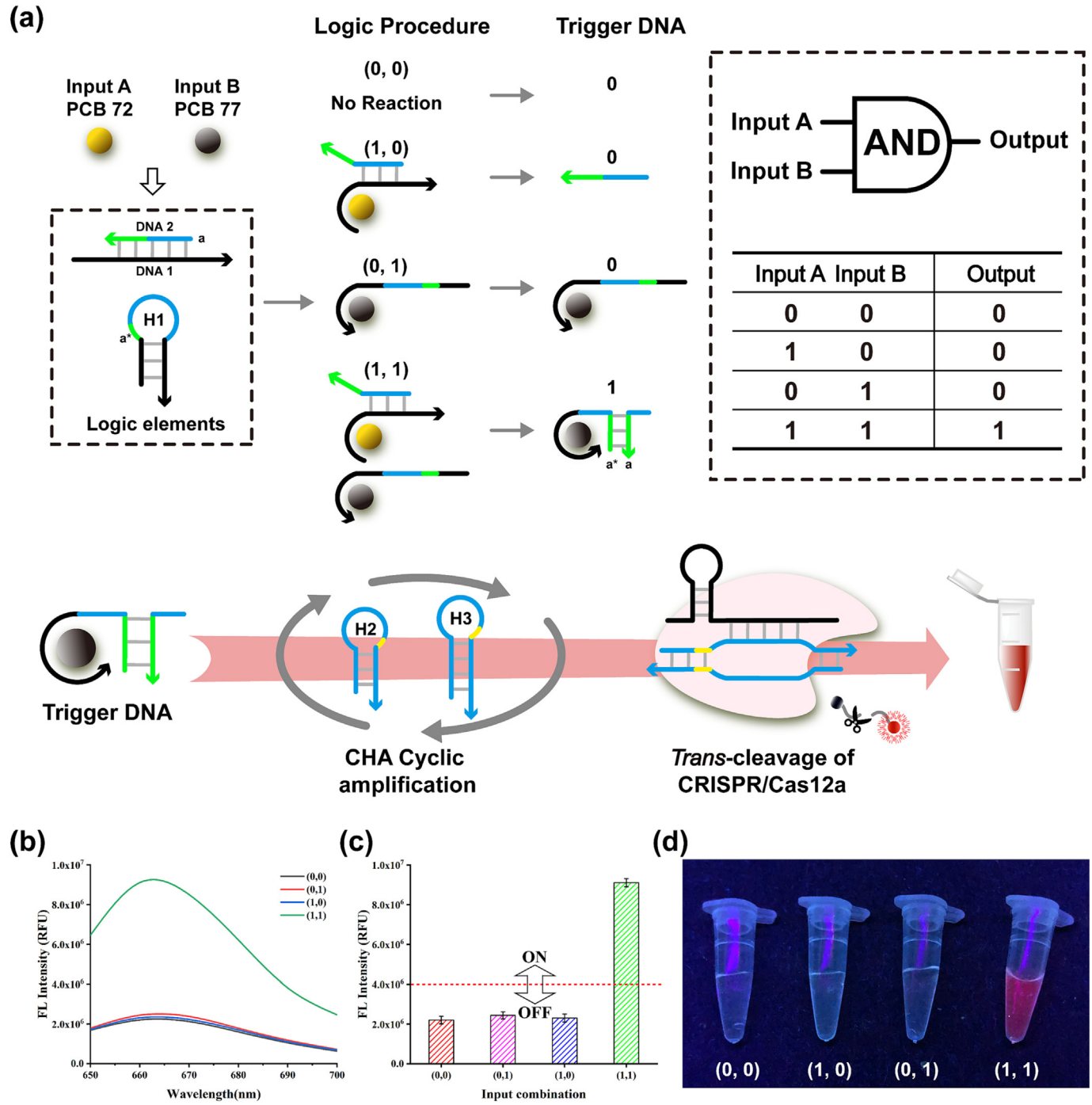

Fig. 4. (a) Schematic illustration of the AND gate using PCB72 and PCB77 as inputs. Inset: The truth table of the AND logic gate. (b) Fluorescence spectra of the AND logic gate. (c) Column diagram of the corresponding fluorescence intensities at 665 nm. The red dashed line shows the threshold value of 4.0×10^6. (d) The colorimetric responses of the AND logic gate with the input combinations of (0,0), (1,0), (0,1), and (1,1), respectively.

intensities at 665 nm of the logic gate were shown in Fig. 5b and c, respectively. The colorimetric signal output of the INHIBIT logic gate was shown in Fig. 5d. In INHIBIT logic operation, the output is 1 only if one input is 1; otherwise, the output is 0.

4. Conclusions

In conclusion, we have successfully developed a biocomputing platform based on hairpin probe assembly and CRISPR/Cas12a. Through the rational design of the sensing DNA probes, the YES, OR, AND, and INHIBIT logic gates were constructed for the intelligent detection of PCB72 and PCB77. The linear range for PCB72 is from 500 fg/mL to 50 ng/mL and the LOD is 128 fg/mL (S/N = 3). Recovery experiments in real water samples show that the recovery rates range from 94 % to 106 % and the relative standard deviations (RSD) are in the range of 2.0–6.8 %. The logic sensing platform exhibits good specificity and the nontarget molecules did not interfere with the test results. In the OR logic gate, the input combinations of (0,1), (1,0), and (1,1) can generate an output of 1. In the AND logic gate, only in the presence of both inputs (1,1) can give an output of 1. In the INHIBIT logic gate, the output is 1 only if the input combination is (1,0). The logic results can be directly observed by the naked-eye under a portable UV lamp. With the advantages of simple operation, user-

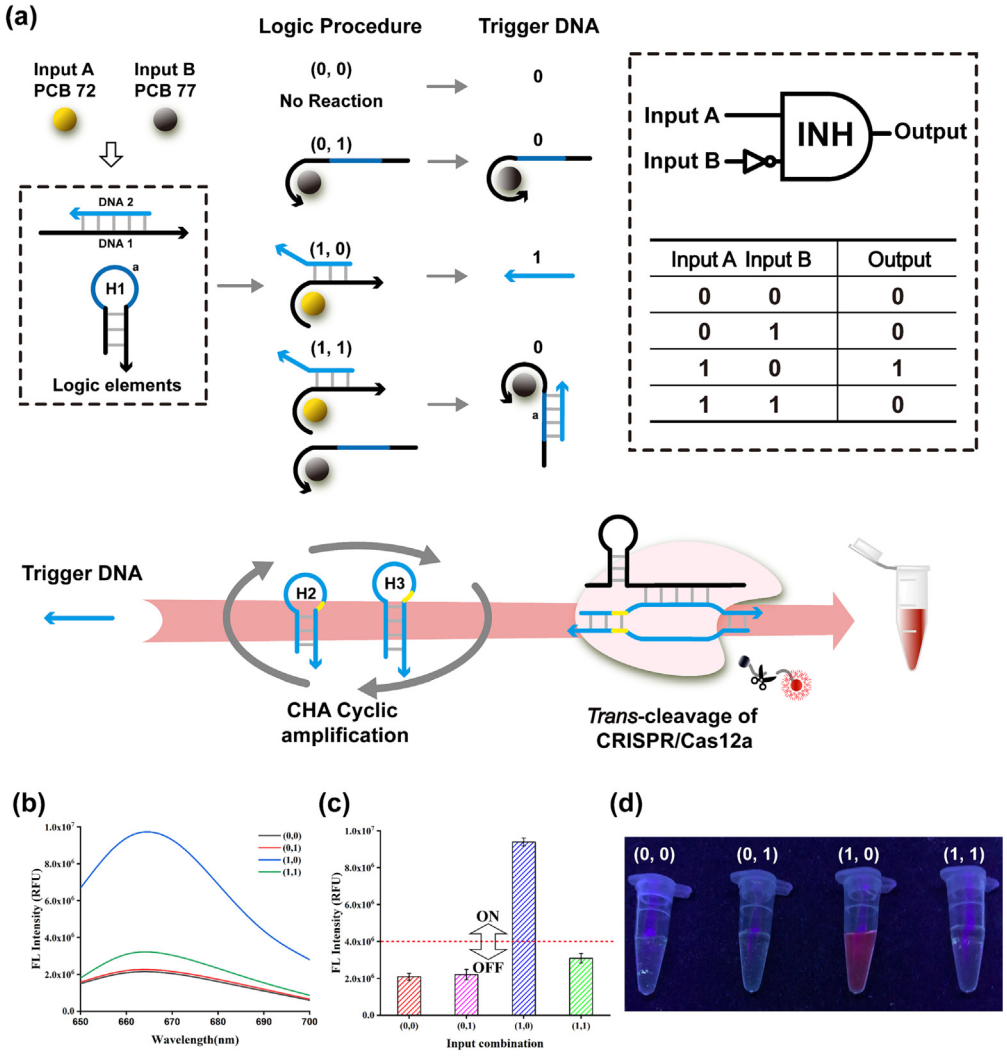

Fig. 5. (a) Schematic illustration of the INHIBIT gate using PCB72 and PCB77 as inputs. Inset: The truth table of the INHIBIT logic gate. (b) Fluorescence spectra of the INHIBIT logic gate. (c) Column diagram of the corresponding fluorescence intensities at 665 nm. The red dashed line shows the threshold value of 4.0×10^6. (d) The colorimetric responses of the INHIBIT logic gate with the input combinations of (0,0), (1,0), (0,1), and (1,1), respectively.

friendliness, signal visualization, and high sensitivity and selectivity, the logic biosensor can be used for on-site and intelligent detection of PCBs in complex samples.

CRediT authorship contribution statement

Fang Deng: Conceptualization, Methodology, Data curation, Writing – original draft. **Jiafeng Pan:** Methodology, Validation. **Manjia Chen:** Data curation, Methodology, Validation. **Zhi Liu:** Methodology, Validation, Supervision. **Junhua Chen:** Conceptualization, Supervision, Funding acquisition, Project administration, Writing – review & editing. **Chengshuai Liu:** Supervision, Funding acquisition, Project administration, Writing – review & editing.

Data availability

Data will be made available on request.

Declaration of competing interest

The authors declare that they have no known competing financial interests or personal relationships that could have appeared to influence the work reported in this paper.

Acknowledgements

This study was financially supported by the Guangdong Laboratory for Lingnan Modern Agriculture Research Project (NZ2021026) and GDAS' Project of Science and Technology Development (2022GDASZH-2022010105).

Appendix A. Supplementary data

Supplementary data to this article can be found online at https://doi.org/10.1016/j.scitotenv.2023.163465.

References

Andrew, A., Zhou, J., Gui, J., Harrison, A., Shi, X., Li, M., Guetti, B., Nathan, R., Tischbein, M., Pioro, E., Stommel, E., Bradley, W., 2022. Airborne lead and polychlorinated biphenyls (PCBs) are associated with amyotrophic lateral sclerosis (ALS) risk in the U.S. Sci. Total Environ. 819, 153096.

Cao, H., Mao, K., Ran, F., Xu, P., Zhao, Y., Zhang, X., Zhou, H., Yang, Z., Zhang, H., Jiang, G., 2022. Paper device combining CRISPR/Cas12a and reverse-transcription loop-mediated isothermal amplification for SARS-CoV-2 detection in wastewater. Environ. Sci. Technol. 56, 13245–13253.

Chen, J., Pan, J., Liu, Z., 2020. Versatile sensing platform for Cd2+ detection in Rice samples and its applications in logic gate computation. Anal. Chem. 92, 6173–6180.

Chen, J., Shi, G., Yan, C., 2021. Visual test paper for on-site polychlorinated biphenyls detection and its logic gate applications. Anal. Chem. 93, 15438–15444.
Cheng, R., Liu, S., Shi, H., Zhao, G., 2018. A highly sensitive and selective aptamer-based colorimetric sensor for the rapid detection of PCB 77. J. Hazard. Mater. 341, 373–380.
Christensen, K., Carlson, L.M., Lehmann, G.M., 2021. The role of epidemiology studies in human health risk assessment of polychlorinated biphenyls. Environ. Res. 194, 110662.
Deng, F., Pan, J., Liu, Z., Chen, J., 2023. Cascaded molecular logic gates using antibiotics as inputs based on exonuclease III and DNAzyme. Talanta 252, 123832.
Ding, X., Yin, K., Li, Z., Lalla, R.V., Ballesteros, E., Sfeir, M.M., Liu, C., 2020. Ultrasensitive and visual detection of SARS-CoV-2 using all-in-one dual CRISPR-Cas12a assay. Nat. Commun. 11, 4711.
Dronina, J., Samukaite-Bubniene, U., Ramanavicius, A., 2021a. Advances and insights in the diagnosis of viral infections. J. Nanobiotechnology. 19 (1), 348.
Dronina, J., Samukaite-Bubniene, U., Ramanavicius, A., 2021b. The application of DNA polymerases and Cas9 as representative of DNA-modifying enzymes group in DNA sensor design (review). Biosens. Bioelectron. 175, 112867.
Dronina, J., Samukaite-Bubniene, U., Ramanavicius, A., 2022. Towards application of CRISPR-Cas12a in the design of modern viral DNA detection tools (Review). J. Nanobiotechnology. 20 (1), 41.
Erbas-Cakmak, S., Kolemen, S., Sedgwick, A.C., Gunnlaugsson, T., James, T.D., Yoon, J., Akkaya, E.U., 2018. Molecular logic gates: the past, present and future. Chem. Soc. Rev. 47, 2228.
Fan, L., Zhang, C., Shi, H., Zhao, G., 2019. Design of a simple and novel photoelectrochemical aptasensor for detection of 3,3',4,4'-tetrachlorobiphenyl. Biosens. Bioelectron. 124–125, 8–14.
Feng, C., Chen, T., Mao, D., Zhang, F., Tian, B., Zhu, X., 2020. Construction of a ternary complex based DNA logic nanomachine for a highly accurate imaging analysis of cancer cells. ACS Sens. 5, 3116–3123.
Feng, W., Newbigging, A.M., Tao, J., Cao, Y., Peng, H., Le, C., Wu, J., Pang, B., Li, J., Tyrrell, D.L., Zhang, H., Le, X.C., 2021. CRISPR technology incorporating amplification strategies: molecular assays for nucleic acids, proteins, and small molecules. Chem. Sci. 12, 4683–4698.
Gao, G., Chen, H., Dai, J., Jin, L., Chai, Y., Zhu, L., Liu, X., Lu, C., 2020. Determination of polychlorinated biphenyls in tea using gas chromatography-tandem mass spectrometry combined with dispersive solid phase extraction. Food Chem. 316, 126290.
Ge, L., Wang, W., Sun, X., Hou, T., Li, F., 2016. Versatile and programmable DNA logic gates on universal and label-free homogeneous electrochemical platform. Anal. Chem. 88, 9691–9698.
Hu, Y., Cheng, H., 2013. Application of stochastic models in identification and apportionment of heavy metal pollution sources in the surface soils of a large-scale region. Environ. Sci. Technol. 47, 3752–3760.
Huang, Y., Liu, Y., Du, P., Zeng, L., Mo, Ce, Li, Y., Lü, H., Cai, Q., 2019. Occurrence and distribution of antibiotics and antibiotic resistant genes in water and sediments of urban rivers with black-odor water in Guangzhou South China. Sci. Total Environ. 670, 170–180.
Jiang, Y., Hu, M., Liu, A., Lin, Y., Liu, L., Yu, B., Zhou, X., Pang, D., 2021. Detection of SARS-CoV-2 by CRISPR/Cas12a-enhanced colorimetry. ACS Sens. 6, 1086–1093.
Kaminski, M.M., Abudayyeh, O.O., Gootenberg, J.S., Zhang, F., Collins, J.J., 2021. CRISPR-based diagnostics. Nat. Biomed. Eng. 5, 643–656.
Lammel, T., Wassmur, B., Mackevica, A., Chen, C.E.L., Sturve, J., 2019. Mixture toxicity effects and uptake of titanium dioxide (TiO 2) nanoparticles and 3,3',4,4'-tetrachlorobiphenyl (PCB77) in juvenile brown trout following co-exposure via the diet. Aquat. Toxicol. 213, 105195.
Li, S., Cheng, Q., Wang, J., Li, X., Zhang, Z., Gao, S., Cao, R., Zhao, G., Wang, J., 2018. CRISPR-Cas12a-assisted nucleic acid detection. Cell Discov. 4, 18–21.
Li, Y., Deng, F., Hall, T., Vesey, G., Goldys, E.M., 2021. CRISPR/Cas12a-powered immunosensor suitable for ultra-sensitive whole cryptosporidium oocyst detection from water samples using a plate reader. Water Res. 203, 117553.
Liu, L., Duan, J., Wei, X., Hu, H., Wang, Y., Jia, P., Pei, D., 2022. Generation and application of a novel high-throughput detection based on RPA-CRISPR technique to sensitively monitor pathogenic microorganisms in the environment. Sci. Total Environ. 838, 156048.
Melymuk, L., Blumenthal, J., Sáňka, O., Shu-Yin, A., Singla, V., Šebková, K., Fedinick, K.P., Diamond, M.L., 2022. Persistent problem: global challenges to managing PCBs. Environ. Sci. Technol. 56, 9029–9040.
Miao, P., Tang, Y., 2021. Cascade Strand displacement and bipedal walking based DNA logic system for miRNA diagnostics. ACS Cent. Sci. 7, 1036–1044.
Nguyen, L.T., Smith, B.M., Jain, P.K., 2020. Enhancement of trans-cleavage activity of Cas12a with engineered crRNA enables amplified nucleic acid detection. Nat. Commun. 11, 4906.
Pan, J., Deng, F., Chen, J., 2023. A fluorescent biosensor for Cd2+ detection in water samples based on Cd2+-fueled wheel DNAzyme walker and its logic gate applications. Sci. Total Environ. 864, 161046.
Shen, H., Qileng, A., Yang, H., Liang, H., Zhu, H., Liu, Y., Lei, H., Liu, W., 2021. "Dual-signal-On" integrated-type biosensor for portable detection of miRNA: Cas12a-induced photoelectrochemistry and fluorescence strategy. Anal. Chem. 93, 11816–11825.
Sun, M., Li, R., Zhang, J., Yan, K., Liu, M., 2019. One-pot synthesis of a CdS-reduced graphene oxide-carbon nitride composite for self-powered photoelectrochemical aptasensing of PCB72. Nanoscale 11, 5982–5988.
Tang, Y., Gao, L., Feng, W., Guo, C., Yang, Q., Li, F., Le, X.C., 2021. The CRISPR-cas toolbox for analytical and diagnostic assay development. Chem. Soc. Rev. 50, 11844–11869.
Tregubov, A.A., Nikitin, P.I., Nikitin, M.P., 2018. Advanced smart nanomaterials with integrated logic-gating and biocomputing: Dawn of theranostic nanorobots. Chem. Rev. 118, 10294–10348.
Wang, Y., Bai, J., Huo, B., Yuan, S., Zhang, M., Sun, X., Peng, Y., Li, S., Wang, J., Ning, B., Gao, Z., 2018. Upconversion fluorescent aptasensor for polychlorinated biphenyls detection based on nicking endonuclease and hybridization chain reaction dual-amplification strategy. Anal. Chem. 90, 9936–9942.
Wang, F., Lv, H., Li, Q., Li, J., Zhang, X., Shi, J., Wang, L., Fan, C., 2020. Implementing digital computing with DNA-based switching circuits. Nat. Commun. 11, 121.
Xiong, Y., Zhang, J., Yang, Z., Mou, Q., Ma, Y., Xiong, Y., Lu, Y., 2020. Functional DNA regulated CRISPR-Cas12a sensors for point-of-care diagnostics of non-nucleic-acid targets. J. Am. Chem. Soc. 142 (2020), 207–213.
Xiong, E., Jiang, L., Tian, T., Hu, M., Yue, H., Huang, M., Lin, W., Jiang, Y., Zhu, D., Zhou, X., 2021. Simultaneous dual-gene diagnosis of SARS-CoV-2 based on CRISPR/Cas9-mediated lateral flow assay. Angew. Chem. Int. Ed. 60, 5307–5315.
Xu, M., Gao, Y., Wang, X., Han, X., Zhao, B., 2021. Comprehensive strategy for sample preparation for the analysis of food contaminants and residues by GC-MS/MS: a review of recent research trends. Foods. 10, 2473.
Yi, K., Zhang, X., Zhang, L., 2021. Smartphone-based ratiometric fluorescent definable system for phosphate by merged metal−organic frameworks. Sci. Total Environ. 772, 144952.
Yu, Y., Guo, Q., Jiang, W., Zhang, H., Cai, C., 2021. Dual-aptamer-assisted AND logic gate for cyclic enzymatic signal amplification electrochemical detection of tumor-derived small extracellular vesicles. Anal. Chem. 93, 11298–11304.
Yue, H., Shu, B., Tian, T., Xiong, E., Huang, M., Zhu, D., Sun, J., Liu, Q., Wang, S., Li, Y., Zhou, X., 2021. Droplet Cas12a assay enables DNA quantification from unamplified samples at the single-molecule level. Nano Lett. 21, 4643–4653.
Zhang, B., Tian, P., Zhu, H., Xie, L., Dai, P., He, B., 2021. Ultrasensitive detection of PCB77 based on exonuclease III-powered DNA walking machine. J. Hazard. Mater. 416, 125831.
Zhang, C.Y., Li, X., Stietz, K.P.K., Sethi, S., Yang, W., Marek, R.F., Ding, X., Lein, P.J., Hornbuckle, K.C., Lehmler, H.J., 2022. Machine learning-assisted identification and quantification of hydroxylated metabolites of polychlorinated biphenyls in animal samples. Environ. Sci. Technol. 56, 13169–13178.
Zhang, H., Huang, Z., Liu, Y., Hu, L., He, L., Liu, Y., Zhao, J., Ying, G., 2023. Occurrence and risks of 23 tire additives and their transformation products in an urban water system. Environ. Int. 171, 107715.
Zhou, R., Li, Y., Dong, T., Tang, Y., Li, F., 2020. A sequence-specific plasmonic loop-mediated isothermal amplification assay with orthogonal color readouts enabled by CRISPR Cas12a. Chem. Commun. 56, 3536–3538.